Effect of retroreflection on a Fizeau phase-shifting interferometer

Chiayu Ai and James C. Wyant

Phase errors in a Fizeau phase-shifting interferometer caused by multiple-reflected beams from a retroreflective optics, such as a corner cube and a right-angle prism, are studied. Single- and double-pass configurations are presented, and their measurement results are compared. An attenuator is not needed in a double-pass configuration because light is reflected by the retroreflective optics twice and the reference surface once and hence the intensities match. It is more accurate to test a corner cube or a right-angle prism in a double-pass configuration than in a single-pass configuration. Simulations and experimental results are presented.

Key words: Optical testing, retroreflection, corner cube, phase-shifting interferometry.

Introduction

Spurious reflections normally introduce errors into the measurement results obtained with phase-shift interferometry.[1–6] This error has a spatial frequency equal to the sum of the spatial frequencies of the main fringes and the ghost fringes, or their difference.[4] If a test surface, such as a mirror or a corner cube, is highly reflective compared with the reference surface, then the spurious reflection problem becomes more complicated and causes the intensity mismatches and the multiple reflections between the test sample and the interferometer. In the case of multiple reflections, Hariharan[3] points out that if a four-frame phase calculation algorithm is used, the phase error caused by the multiple reflection is eliminated to a first-order approximation. Bonsch and Bohme[5] give a new algorithm that can completely eliminate the phase error (mainly quadruple frequency) because of the multiple reflections of a mirror.

While using a Fizeau interferometer, it is common practice for one to reduce the reflection of a highly reflective test sample by adding an attenuator in front of it. During the testing of a corner cube, it was discovered that there is a single-frequency error that has the same spatial frequency as that of the main interference fringes. But, when we used the same interferometer this single-frequency error was not observed for either an uncoated surface or a low-reflection mirror. In a phase-shifting interferometer it is not unusual to see it double-frequency error, which is commonly caused by a piezoelectric transducer (PZT) calibration error.[2] All these indicated that the PZT was well calibrated in the experiment and that this error for a corner cube was not caused by the PZT calibration error. The reflection of a corner cube is different from that of a mirror. For a corner cube not only are there multiple reflections but also retroreflection. Because the phase error caused by multiple reflections of a mirror is eliminated to a first-order approximation,[3] this single-frequency error for a corner cube must be caused by the retroreflection of a corner cube.

First, we derive the formula of a three-beam approximation for the multiple reflection of a low-reflection mirror tested with a Fizeau phase-shifting interferometer. The formula shows that for a mirror the effect of multiple reflections is canceled. But this is not true for a corner cube. For simplicity, we derive the formula for retroreflection of a right-angle prism. Because both the prism and the cube have retroreflection, the formula can apply to the cube. The formula shows that the multiple reflection of a corner cube introduces errors into the measurement result. We further investigate the problem by using different attenuators to control the effective reflectance of the samples and hence the multiple reflections. We present the results of the experiments performed with a flat mirror, a right-angle prism, and a corner cube. The cube is tested in both single- and double-pass configurations.

The authors are with Wyko Corporation, 2650 E. Elvira Road, Tucson, Arizona 85706.

Received 6 February 1992.
0003-6935/93/193470-09$06.00/0.

Multiple Reflections of a Mirror

In practice, the intensities of the two beams from the test and the reference surfaces may be the same or may be within a magnitude of 10 to each other. In this paper we deal only with the situation in which the effective reflectance of the test surface, R_2, is several times the effective reflectance of the reference surface, R_1. Here we assume that $R_2 \leq 50\%$ and $R_1 = 4\%$. In this section the multiple reflection between two surfaces with different reflectances are presented without approximation, and the four-frame phase calculation algorithm is used in the phase-error analysis. Then a three-beam model is presented. The results show that for the three-beam model the phase errors caused by multiple reflections are eliminated.

The amplitudes of the beams of multiple reflections between the reference and the test surfaces are shown in Fig. 1. It can be shown without any approximation that the normalized intensity is equal to

$$I_r/I_i = [(r_1 - r_2)^2 + 4r_1r_2 \sin^2(\delta/2)] / [(1 - r_1r_2)^2 + 4r_1r_2 \sin^2(\delta/2)], \quad (1)$$

where I_r and I_i are the intensities of the reflected and the incident beams, respectively, and $\delta/2 = 2\pi d/\lambda$, in which d is the distance between the test and the reference surface. r_1 and r_2 are the coefficients of reflection of the reference (top) and the test (bottom) surfaces, respectively, and hence $r_1 = R_1^{1/2}$ and $r_2 = R_2^{1/2}$. In a Fizeau phase-shifting interferometer the reference surface is translated by a PZT to introduce a proper phase shift. Because of reflection the reference surface is shifted by $\lambda/8$ between each step to give a phase shift of $-90°$. From the four-frame phase calculation algorithm,[7] the resulting phase is given as

$$\text{phase} = \tan^{-1}[(I_3 - I_1)/(I_0 - I_2)] \quad (2)$$

where I_{0-3} are the intensities of the four frames obtained from Eq. (1) for $\Delta\delta = -90°$. When we use Eq. (2), the modulation of the intensity during the phase shifting is defined as

$$\text{modulation} = \text{ac/dc} = \{0.5[(I_3 - I_1)^2 + (I_0 - I_2)^2]^{1/2}\} / \{(I_0 + I_1 + I_2 + I_3)/4\}, \quad (3)$$

where ac and dc correspond, respectively, to the numerator and the denominator in the right-hand side. When we use Eq. (1), the modulation can be expressed as a function of r_1, r_2 and the initial phase δ. It can be shown that the modulation varies slightly for different initial phases. The numerator and the denominator represent the ac and the dc parts of a modulated signal, respectively. Figures 2(a) and 2(b) are the intensity profile and the phase error for the initial phases from 0° to 360°, respectively, for various R_1 and R_2. The dotted curve in Fig. 2(a) is the best-fit sinusoidal curve to the intensity profile. When two surfaces have different reflectances, the modulation is less than the unity and the intensity is no longer sinusoidal. The phase error caused by multiple reflection has a spatial frequency of four times that of the main interference fringes, and this error is small and negligible as shown in Fig. 2(b). Table 1 lists the phase error, the modulation, the dc

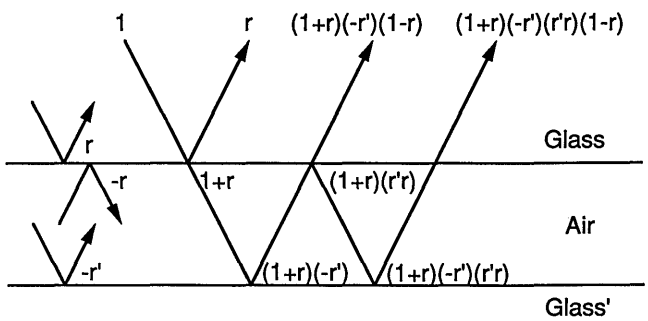

Fig. 1. Multiple reflection between the reference (top) and the test (bottom) surfaces. r and r' are the coefficients of the reflection of the two surfaces ($r = r_1$ and $r' = r_2$).

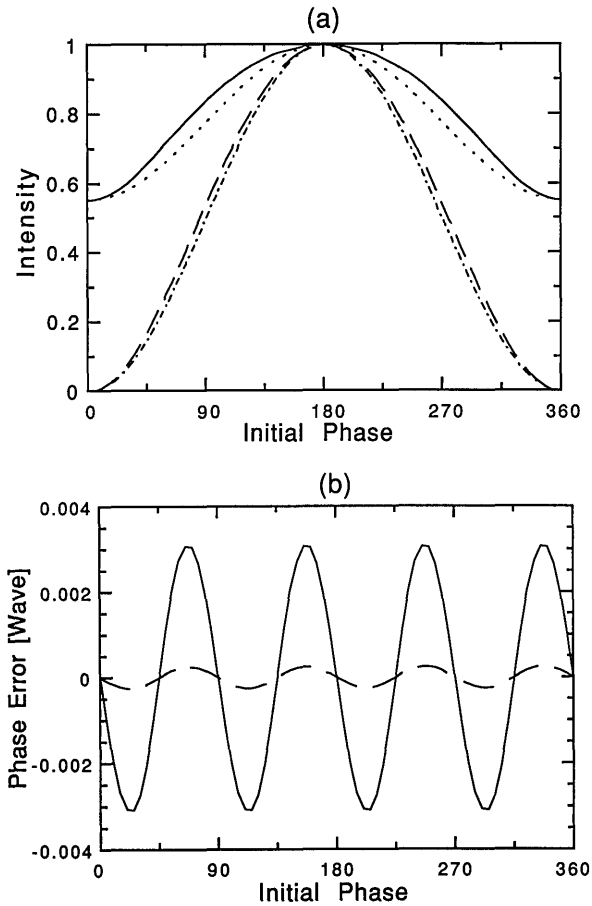

Fig. 2. (a) Intensity profile and (b) phase error for the initial phase from 0° to 360°. The solid curve is for $R_1 = 4\%$ and $R_2 = 50\%$ and the dashed curve is for $R_1 = 4\%$ and $R_2 = 4\%$. The intensities are derived from Eq. (1), and the dotted curves are the best-fit sinusoidal curves.

Table 1. Characteristics for Different Reflectances of the Test Sample

R_2	Phase Error (pv)	Modulation	dc of Eq. (3)	ac of Ec. (3)
4%	0.0005λ	0.958–0.962	0.077	0.073–0.074
16%	0.0020λ	0.685–0.694	0.188	0.129–0.131
25%	0.0031λ	0.528–0.539	0.273	0.144–0.147
36%	0.0045λ	0.391–0.403	0.377	0.147–0.152
50%	0.0062λ	0.266–0.277	0.510	0.136–0.141

and the ac terms of Eq. (3) for different reflectances of the test sample, obtained using the four-frame phase calculation algorithm where the intensities are derived from Eq. (1) for $R_1 = 4\%$. Because of reflection, the surface error equals one half of the phase error. This clearly shows that the effect of the multiple reflections is negligible, if R_2 is only several times of R_1. Although it can be shown that for a higher reflectance R_2 the phase error that is due to the multiple reflection is still negligible, the fringe contrast further decreases. The low contrast becomes a more important error source than the multiple reflection, and the phase is difficult to measure accurately. In Table 1, if R_1 is quadrupled, then the phase error is approximately quadrupled. In the following, we limit R_1 equal to 4% and R_2 less than 50%.

A three-beam approximation is presented below to help understand the effect of the multiple reflections on the phase-shifting interferometer. Figure 3 is a schematic of a Fizeau phase-shifting interferometer with a laser source at 633 nm. The two surfaces of the transmission flat, whose refractive index n, are the reference surface (R) and the antireflective surface (AR). The coefficients of reflection of the reference surface (R) and the test surface (T) are r_1 and r_2, respectively. The three returned beams are r, t, and s, respectively. The amplitude of the beam reflected by the reference surface is

$$r_1 \exp \mathbf{i}[\phi_i(x) + 2n\phi_r(x) + \eta], \tag{4}$$

where η is the phase shift introduced by the PZT and $\phi_r(x)$ is the surface contribution of the reference surface. The factor $2n$ is due to internal reflection. $\phi_i(x)$ is the wave front at the output aperture of the Fizeau interferometer and hence represents the system aberration. Similarly, the amplitudes of the first- and second-reflected beams by the test surface are

$$(1 + r_1)(-r_2)(1 - r_1) \times \exp \mathbf{i}[\phi_i(x) + 2(n - 1)\phi_r(x) + 2\phi_t(x)], \tag{5}$$

$$(1 + r_1)(-r_2)(1 - r_1)r_1r_2 \exp \mathbf{i}[\phi_i(x) + 2(n - 1)\phi_r(x) + 4\phi_t(x) - 2\phi_r(x) - \eta)], \tag{6}$$

respectively, where $\phi_t(x)$ is the contribution of the test surface, i.e., the test-surface profile plus the distance between two surfaces. The minuses for $\phi_r(x)$ and η are due to the back reflection of the reference surface, and $2(n - 1)\phi_r(x)$ is due to the transmission of the reference surface. When a factor of $\exp \mathbf{i}[2(n - 1)\phi_r(x)]$ is extracted from each of the three beams, the complex amplitudes of the three beams can be simplified and are given as follows:

$r_1 \exp \mathbf{i}[\phi_i(x) + 2\phi_r(x) + \eta]$ from the reference surface,

$-(1 - R_1)r_2 \exp \mathbf{i}[\phi_i(x) + 2\phi_t(x)]$ from the first reflection of the test surface,

$-(1 - R_1)r_2(r_1r_2)\exp \mathbf{i}[\phi_i(x) + 4\phi_t(x) - 2\phi_r(x) - \eta]$ from the secondary reflection. (7)

Therefore the intensity of the three-beam interference is

$$I = C + D\cos[2\phi_t(x) - 2\phi_r(x) - \eta] + E\cos[4\phi_t(x) - 4\phi_r(x) - 2\eta] + F\cos[2\phi_t(x) - 2\phi_r(x) - \eta], \tag{8}$$

where

$$C = r_1^2 + (1 - R_1)^2r_2^2 + (1 - R_1)^2r_2^4r_1^2,$$
$$D = -2(1 - R_1)(r_1r_2),$$
$$E = -2(1 - R_1)(r_1r_2)^2,$$
$$F = 2(1 - R_1)^2r_2^2(r_1r_2).$$

It should be noted that the system aberration $\phi_i(x)$ is cancelled. This is why the system aberration of a Fizeau interferometer is not critical. When the reference surface is shifted to introduce a phase shift of $-90°$ between each step, the intensities of four frames are obtained with $\eta = 0°$, $-90°$, $-180°$, and $-270°$, respectively. When the four intensities are substituted into Eq. (2), it is clear that the third term $E\cos(4\phi_t - 4\phi_r)$ is canceled in the subtraction operation and the resulting phase equals $2(\phi_t - \phi_r)$. Hence, for the three-beam approximation the phase error caused by multiple reflections is eliminated

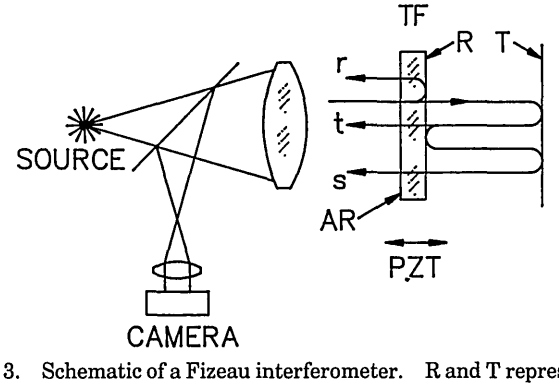

Fig. 3. Schematic of a Fizeau interferometer. R and T represent the reference and the test surfaces, respectively, and the three beams reflected by them are r, t, and s. These notations are also used in Figs. 4 and 5.

completely. Although the derivation above is different from Hariharan's, both have the same result. He pointed out that, if a four-frame phase calculation algorithm is used, the phase error caused by multiple reflections of a mirror is eliminated to the first-order approximation.[3] However, if there is a corner cube, the result is different. Although a new algorithm given by Bonsch and Bohme[5] can completely eliminate the phase error (mainly quadruple frequency) introduced by the multiple reflections of a mirror, neither this nor the four-frame algorithm can remove the single-frequency error caused by the multiple reflections of a retroreflector. In the next section, using the three-beam approximation, we are able to explain this error and propose a method to reduce this error.

To justify the three-beam model, the values of C, D, E, and F of Eq. (8) are listed in Table 2, for $R_1 = 4\%$ and various R_2. Because both D and F terms of Eq. (8) have the same argument in the trigonometric function, they can be added together. The opposite signs of D and F mean that they interfere destructively. When we compare Table 2 with Table 1, it can be seen that $C \approx$ dc of Eq. (3) and $D + F \approx$ ac of Eq. (3). Therefore, to the second order, Eqs. (7) and (8) are good approximations of the electric field and the intensity of the multiple reflection, respectively, for a phase-shifting interferometry.

Retroreflections of a Right-Angle Prism

In this section we use the three-beam approximation to derive the wave-front formulas reflected by a retroreflector. To ensure that the interference can be approximated as a three-beam interference, an attenuator is inserted to make the effective reflectance of the retroreflector less than 50%. Thus the derivation in the previous section can be applied here. For simplicity, we use a right-angle prism, instead of a corner cube, to derive the wave-front formula when both retroreflection and multiple reflections occur. At the end of this section we present a double-pass configuration where multiple reflections can be negligible.

Figure 4(a) shows the lower portion of the test beam (t) reflected by the prism. This test beam, i.e., the output beam ϕ_{out} from the first reflection, is given as follows:

$$\phi_{out}(-x) = \phi_{in}(x) + \phi_p(x) + \phi_p(-x), \qquad \text{if } x > 0, \quad (9)$$

where ϕ_p is the contribution from one half of the prism and ϕ_{in} is the phase of the incident beam that

Table 2. Values of C, D, E, and F

R_2	C	D	E	F	$D+F$
4%	0.0769	−0.0768	−0.0031	0.0029	−0.0739
16%	0.1884	−0.1536	−0.0123	0.0236	−0.1300
25%	0.2727	−0.1920	−0.0192	0.0461	−0.1459
36%	0.3766	−0.2304	−0.0277	0.0796	−0.1508
50%	0.5100	−0.2715	−0.0384	0.1303	−0.1412

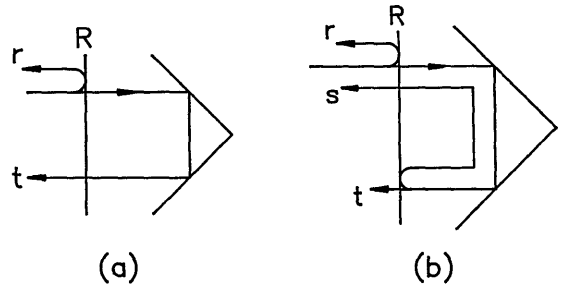

Fig. 4. (a) Lower portion of test beam t reflected by a right-angle prism. (b) Multiple reflections in the single-pass configuration. s is the secondary reflection by the prism, and r is the reference beam.

equals the aberration of the wave front at the output aperture of the interferometer. If we define the ray direction at the output aperture of the interferometer as the interferometer axis, then $\phi_{in}(x)$ has no tilt, although it may still include focus, coma, etc. It can be shown that Eq. (9) is also valid for $x < 0$. Thus, by defining an operator $\mathbf{O}$, which flips the sign of the coordinates, we can express the test beam, i.e., the output wave front ϕ_{out} from the first reflection, as

$$\begin{aligned}\phi_{out}(x) &= \mathbf{O}[\phi_{in}(x) + \phi_p(x) + \phi_p(-x)] \\ &= \phi_{in}(-x) + \phi_p(x) + \phi_p(-x) \qquad (10)\end{aligned}$$

for both $x > 0$ and $x < 0$. Because this equation includes both $\phi_p(x)$ and $\phi_p(-x)$, the contribution of a right-angle prism must be an even function. Here we define $\phi_{t,e}(x)$ to represent the total contribution from both halves of the prism,

$$\phi_{t,e}(x) = \phi_p(x) + \phi_p(-x). \qquad (11)$$

For a corner cube, because of the symmetry about the center of a corner cube, the retroreflection of a cube is an even function for the $\mathbf{r}$ coordinate of a polar coordinate system. Therefore all the derivations for the prism can apply to the cube, by simply replacing $\mathbf{x}$ with $\mathbf{r}$. It is obvious that $\phi_{t,e}(x)$ is an even function and can represent the contribution of a right-angle prism or a corner cube.

Figure 4(b) shows the multiple retroreflections in a single-pass configuration. The new incident beam for the secondary reflection is $\phi_{in}'(x) = \phi_{out}(x) - 2\phi_r(x) - \eta$, where $\phi_{out}(x)$ is the output wave front of the first reflection given in Eq. (10). Similarly, the output wave front $\phi_{out}'(x)$ of the secondary retroreflection can be derived by using Eq. (10). Both $\phi_{in}'(x)$ and $\phi_{out}'(x)$ are listed as follows:

$$\phi_{in}'(x) = \phi_{in}(-x) + \phi_{t,e}(x) - 2\phi_r(x) - \eta, \qquad (12)$$

$$\begin{aligned}\phi_{out}'(x) &= \mathbf{O}\{\phi_{in}'(x) + \phi_{t,e}(x)\} \\ &= \phi_{in}(x) + 2\phi_{t,e}(x) - 2\phi_r(-x) - \eta. \qquad (13)\end{aligned}$$

Thus, from Eqs. (7), (10), and (13) the complex amplitudes of the reference beam, the first reflec-

tions, and secondary reflections are obtained, respectively.

$$r_1 \exp \mathbf{i}[\phi_i(x) + 2\phi_r(x) + \eta]$$

from the reference surface,

$$-(1 - R_1)r_2 \exp \mathbf{i}[\phi_i(-x) + \phi_{t,e}(x)]$$

from the first reflection of the test surface,

$$-(1 - R_1)r_2^2 r_1 \exp \mathbf{i}[\phi_i(x) + 2\phi_{t,e}(x) - 2\phi_r(-x) - \eta]$$

from the secondary reflection. (14)

where $\phi_{in}(x)$ is replaced with $\phi_i(x)$, because $\phi_{in}(x)$ is equal to the wave front at the output aperture of a Fizeau interferometer. The intensity of the multiple-beam interference can be approximately expressed as given below:

$$\begin{aligned} I = {} & C + D\cos[-2\phi_{i,o}(x) + \phi_{t,e}(x) - 2\phi_r(x) - \eta] \\ & + E\cos[2\phi_{t,e}(x) - 4\phi_{r,e}(x) - 2\eta] \\ & + F\cos[2\phi_{i,o}(x) + \phi_{t,e}(x) - 2\phi_r(-x) - \eta], \end{aligned} \quad (15)$$

where C, D, E, and F are the same as those defined in Eq. (8) and $\phi_{t,e}(x)$ is defined in Eq. (11) and is the contribution of the test sample, which is equivalent to $\phi_t(x)$ in Eq. (8). The second subscript of $\phi_{i,o}(x)$ and $\phi_{r,e}$ indicates that they are the odd part of $\phi_i(x)$ and the even part of $\phi_r(x)$, respectively. Comparing Eq. (15) with Eq. (8), we find two differences: (a) In Eq. (15) the arguments of the terms D and F include the odd portion of the system aberration, $\phi_{i,o}(x)$; i.e., the system aberration is not canceled. (b) The reference surface contribution is $\phi_r(x)$ in the D term and $\phi_r(-x)$ in the F term.

From Eq. (15) for $\eta = 0°, -90°, -180°, -270°$ for the four frames, the differences of the four-frame intensities are

$$\begin{aligned} & I_3 - I_1 \\ & = 2D\sin[-2\phi_{i,o}(x) + \phi_{t,e}(x) - 2\phi_{r,e}(x) - 2\phi_{r,o}(x)] \\ & \quad + 2F\sin[2\phi_{i,o}(x) + \phi_{t,e}(x) - 2\phi_{r,e}(x) + 2\phi_{r,o}(x)], \\ & I_0 - I_2 \\ & = 2D\cos[-2\phi_{i,o}(x) + \phi_{t,e}(x) - 2\phi_{r,e}(x) - 2\phi_{r,o}(x)] \\ & \quad + 2F\cos[2\phi_{i,o}(x) + \phi_{t,e}(x) - 2\phi_{r,e}(x) + 2\phi_{r,o}(x)]. \end{aligned} \quad (16)$$

In Eq. (16) the term E is canceled because of the subtraction operation. Because of the discrepancy between the arguments of the trigonometric functions, the phase error obtained with Eq. (16) is much more complicated than that with Eq. (8). Therefore the multiple reflection of a corner cube is different from the multiple reflection of a mirror. For instance, the system aberration is canceled while a mirror is tested with a Fizeau interferometer. On the other hand, for a corner cube the system aberration is not canceled.

If the amplitude of the beam of the secondary reflection is negligible (i.e., $F \ll D$), the resultant phase is equal to $\phi_{t,e}(x) - 2\phi_{i,o}(x) - 2\phi_r(x)$ with an error equal to $2\phi_r(x) + 2\phi_{i,o}(x)$. Because the aberration of a right-angle prism or a corner cube, $\phi_{t,e}(x)$, is always an even function, as explained above, the odd part of the error must be subtracted mathematically from the resultant phase to reduce the measurement error. If the amplitude of the beam of the secondary reflection is not negligible, the situation becomes complicated. Even the tilt of the reference surface can affect the results as explained below and shown in the experiment.

For simplicity, here we assume that the aberration of the interferometer is negligible i.e., $\phi_{i,o}(x) = 0$. So is the reference surface except for the tilt of the reference surface; i.e., $\phi_{r,e}(x)$ = piston and $\phi_{r,o}(x)$ = tilt. Thus the arguments of the trigonometric functions of Eq. (16) have only $\phi_{t,e}(x)$ and $\phi_{r,o}(x)$ left, plus a constant piston. The effect of the tilt of the reference surface on the measurement accuracy is explained for three different tilts, where the tilt of the reference surface is defined with respect to the interferometer axis. (a) If the tilt of the reference surface is zero, $\phi_{r,o}(x) = 0$, then the arguments of the functions in Eq. (16) are the same, and the multiple reflection has no effect. (b) If $2\phi_{r,o}(x) = \phi_{t,e}(x)$, for either $x > 0$ or $x < 0$, the phase of term D is equal to a constant and the main interference fringe, which is formed by the reference and the test beams, is null. The error is approximately equal to $\pm\sin^{-1}(F/D)$. It can be easily shown that the phase error has the same spatial frequency as that of the ghost fringes.[2,4] (c) Similarly, if $2\phi_{r,o}(x) + \phi_{t,e}(x) = 0$, for either $x > 0$ or $x < 0$, the phase of term F is equal to a constant and the main interference pattern has many tilt fringes determined by the phase of term D. Since only the first order of the spurious reflections is considered, both effects b and c have the same magnitude of phase error, and the phase error is a single-frequency error. If the higher order is considered, the errors for effects b and c are different, as shown in the experiment.

Figure 5 shows the reference and the test beams for a prism or a cube tested in a double-pass configuration, where the lower portion of the reference surface is blocked between it and the interferometer. The test beam is reflected by the prism twice and by the

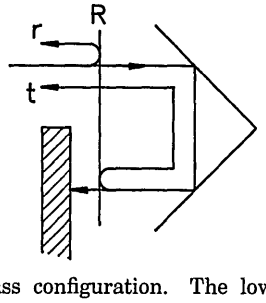

Fig. 5. Double-pass configuration. The lower portion of the reference surface is blocked. r is the reference beam, and t is the test beam, which is reflected by the prism twice and by the reference surface once.

reference surface once. This test beam is equal to the secondary reflection beam in Eq. (14). Because the reference surface is uncoated, any light reflected by the reference surface more than once is negligible. Therefore the double-pass configuration is a two-beam interference situation. Using Eq. (14), we find that the complex amplitudes of the reference and the test beams are given below, respectively,

$$r_1 \exp \mathbf{i}[\phi_i(x) + 2\phi_r(x) + \eta]$$

from the reference surface,

$$-(1 - R_1)r_2^2 r_1 \exp \mathbf{i}[\phi_i(x) + 2\phi_{t,e}(x) - 2\phi_r(-x) - \eta)]$$

from the test surface, (17)

and the intensity of their interference is

$$I = r_1^2 + (1 - R_1)^2 r_2^4 r_1^2 - 2(1 - R_1)r_2^2 r_1^2 \times \cos[2\phi_{t,e}(x) - 4\phi_{r,e}(x) - 2\eta]. \quad (18)$$

If $R_1 = 4\%$ and $R_2 = 92\%$ (i.e., $r_1 = 0.20$ and $r_2 = 0.96$), then both the dc term and the ac coefficientare approximately equal to 7%. Therefore, in the double-pass configuration the fringe contrast is close to unity without using an attenuator. It should be noted that only the even part of the reference wave front, $\phi_{r,e}(x)$, is included in Eq. (18), and hence varying the tilt of the reference surface does not affect the interference fringe pattern. This can be observed in the experiment easily. It should be noted that because of 2η in Eq. (18), for each frame the reference surface is displaced one half of the displacement in the single pass configuration. From Eq. (18), if $\eta = 0°, -45°, -90°$, and $-135°$ for four frames, then the resultant phase is

$$\tan^{-1}[(I_3 - I_1)/(I_0 - I_2)] = 2[\phi_{t,e}(x) - 2\phi_{r,e}(x)]. \quad (19)$$

It should be noted that $\phi_i(x)$ is not included in this equation, and hence the aberration of a Fizeau interferometer has no effect on the measurement. If $\phi_{r,e}(x) = 0$, the prism contribution $\phi_{t,e}(x)$ equals one half of the resultant phase or arctangent value. The double-pass measurement is twice as sensitive as the single-pass measurement.

Experiment

A flat mirror, a right-angle prism, which is composed of two mirrors at 90°, and a hollow corner cube are tested in the experiments. Because the samples are highly reflective, multiple reflections occur. For comparison, the samples are tested with two different attenuators; one with transmission $T = 70\%$, and the other $T = 20\%$. With the Fizeau interferometer, these attenuators give the samples effective reflectances of 50% and 4%, respectively. For the mirror tested with the attenuator of $T = 70\%$ the resultant optical-path difference (OPD) is about 0.007λ rms.

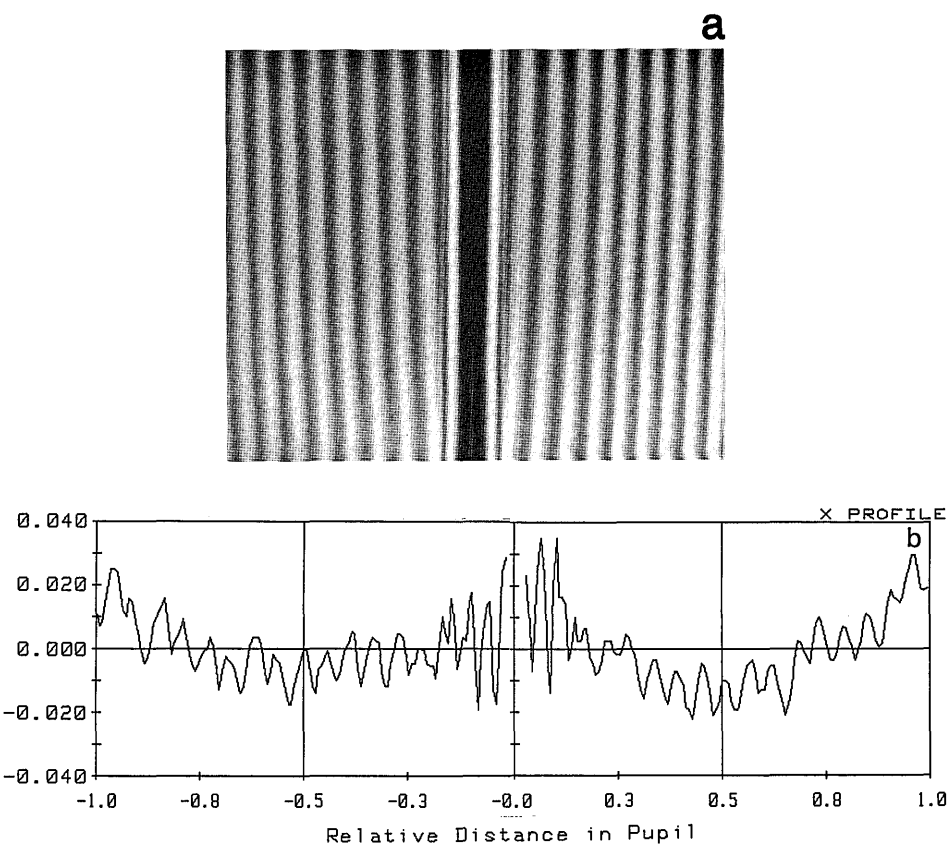

Fig. 6. A right-angle prism tested in a single-pass configuration with an attenuator of $T = 70\%$, where the reference surface is not tilted: (a) interferogram (b) x profile of OPD along the middle of the pupil. The spikes around $x = 0$ are due to diffraction.

On the other hand, while tested with the attenuator of $T = 20\%$, the resultant OPD is about 0.006λ rms. The difference between two resulting phases is within the interferometer noise level. This shows that the effect of the multiple reflection on the measurement result of a mirror is negligible.

Figure 6a is the interferogram of a right-angle prism tested in a single-pass configuration with an attenuator of $T = 70\%$. The reference surface is not tilted at all, and the main interference fringes are evenly distributed in both sides of the pupil. Figure 6b is the x profile of the resultant OPD along the middle of the prism. The ripples are about 0.015λ (peak to valley$-v$) and are a combination of the double- and quadruple-frequency errors. The quadruple-frequency error, which is of interest and much smaller than the double one, is much less than 0.015λ (peak to valley$- v$).

Figure 7 is similar to Fig. 6, but the reference surface is slightly tilted in a direction such that in the right-hand side of the pupil the main interference fringes are vertical and the ghost fringes are horizontal, and vice versa in the left-hand side. (The type of fringes can be distinguished by comparing the fringe contrasts on both sides of the pupil. These horizontal fringes are introduced to show the fringe contrast. During the experiment, there are no horizontal fringes.) There are approximately 17 vertical fringes in each half of the pupil. Figure 7b shows the x profile of the resultant OPD along the middle of the prism; each half has approximately 17 ripples.

A small portion of a 6-in. (15-cm) output aperture of a Fizeau interferometer is used to ensure that the aberrations of the interferometer and the reference surface are negligible except for the tilt of the reference surface. The difference between Figs. 6 and 7 clearly indicates that the tilt of the reference surface has some effects on the measurement. In Fig. 6a the interference fringes are symmetric in both sides of the pupil. The tilt of the reference surface is zero, $\phi_{r,o}(x) = 0$. This was ensured with an accurate corner cube. Therefore the multiple reflection has almost no effect, as shown in Fig. 6b, where the quadruple-frequency error is negligible. In Fig. 7a the main interference fringes are horizontal in the left-hand side and vertical in the right-hand side. From the previous section, along a horizontal line, $2\phi_{r,o}(x) = \phi_{t,e}(x)$ in the left-hand side of the pupil and $2\phi_{r,o}(x) = -\phi_{t,e}(x)$ in the right-hand side. In Fig. 7b the OPD error has the same frequency as that of the interference fringes, i.e., a single-frequency error. The error is ~0.16λ (peak to valley$- v$) as predicted with the three-beam model.[8] The error cannot be explained otherwise. This shows that the three-beam model works reasonably well. In the experiment the pattern of Fig. 7b is swapped, when the tilt of the reference surface is adjusted such that the pattern of Fig. 7a is swapped from left to right. It

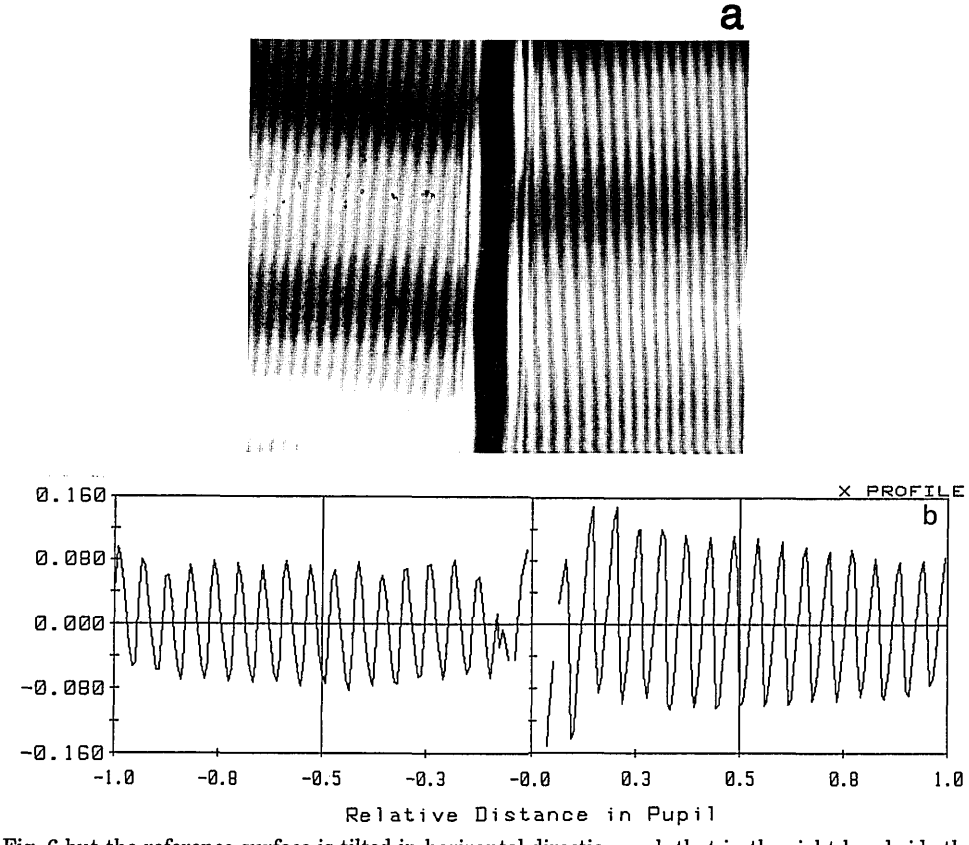

Fig. 7. Same as Fig. 6 but the reference surface is tilted in horizontal direction such that in the right-hand side the main interference fringes are vertical and the ghost fringes are horizontal, and vice versa in the left-hand side.

can also be seen that the frequency of the OPD error varies with the tilt of the reference surface. To explain why the OPD error in the left-hand side is smaller than that in the right, the higher orders of the multiple reflections have to be included. Note that, when an attenuator of $T = 20\%$ is used, the ripples in Fig. 6b disappear, but there still are residual ripples about 0.02λ (peak to valley) in Fig. 7b. Therefore, in a single-pass configuration, it is important to match the intensities of both beams and to align the reference surface properly by obtaining a symmetric interferogram as shown in Fig. 6a.

Figure 8 is the wave-front deformation of a corner cube tested in a single-pass configuration with an attenuator of $T = 20\%$, and hence multiple reflection is negligible. The two isometric contours are obtained before and after mathematically subtracting the odd aberrations of the resultant phases obtained using Eq. (2). Figure 8(a) shows symmetry with respect to the center. The asymmetry should not exist for a corner cube. This indicates that the system aberration of the interferometer is neither cancelled nor negligible. Therefore the odd aberration of the resultant OPD should be removed when the cube is tested in a single-pass configuration.

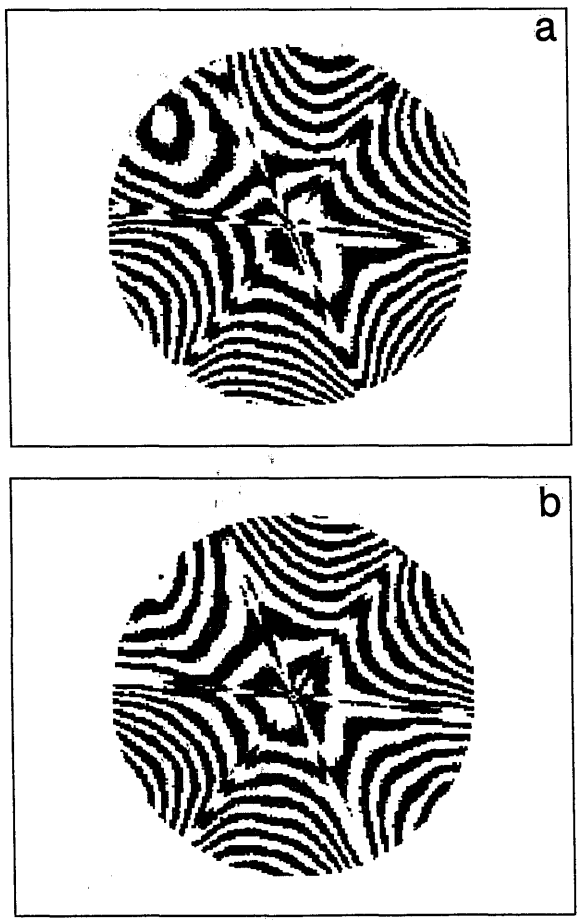

Fig. 8. Isometric contours of the wave-front deformation of a corner cube, tested in a single-pass configuration with an attenuator of $T = 20\%$, (a) before and (b) after the odd aberrations of the resultant OPD's are subtracted. In (a) the contours are asymmetric with respect to the center. (Interval, 0.05λ.)

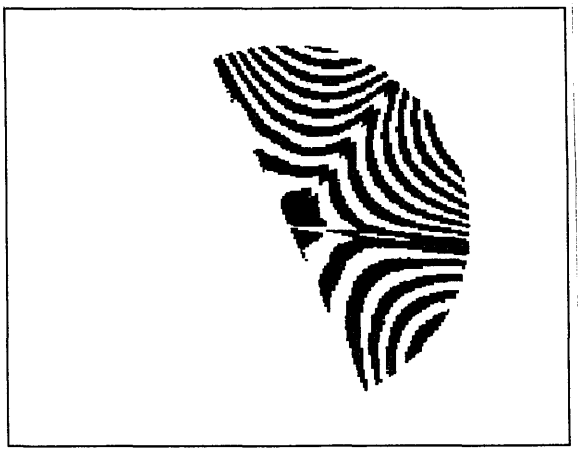

Fig. 9. Isometric contours of the resultant OPD of a corner cube tested in a double-pass configuration without using an attenuator. (Interval, 0.05λ.)

For a double-pass configuration the left-hand side of the pupil of the corner cube does not appear in the interferogram, because the beam is blocked at that portion. Figure 9 is the isometric contours of the resultant OPD of a corner cube tested in a double-pass configuration without using an attenuator. The contrast of the interference fringes is high. This indicates that the intensities of both test and reference beams match. The resultant OPD is obtained using Eq. (19) without substracting any odd aberration. Comparing Fig. 9 with Fig. 8b carefully, one can see that there is no odd aberration in Fig. 9. It means that the system aberration is canceled in the double-pass configuration. In this configuration it is interesting to note that the interferogram pattern does not change when the tilt of the reference surface is adjusted.

Conclusion

When a low-reflection mirror is tested in a Fizeau phase-shifting interferometer, multiple reflections have no effect on the measurement, even though the fringe contrast is no longer sinusoidal. However, this is not true if the multiple reflections include retroreflections of a corner cube or a right-angle prism. For the same R_1 and R_2 the phase error that is due to multiple reflections with a retroreflection is much greater than that without retroreflection. In a single-pass configuration, ideally, light is reflected by the corner cube once. Because of the high reflectance of the corner cube, the intensities of the test and the reference beams do not match. The test beam reflected by the test surface is partially reflected by the reference surface, and multiple reflections occur. Because the wave front is flipped about the center of the cube when it is retroreflected by the cube, the misalignment of the reference surface, such as tilt, results in a ripple in the surface profile and affects the measurement accuracy. If the reference surface is properly aligned, the phase error that is due

to the multiple reflections with retroreflections can be neglected. It should be noted that, even when multiple reflections are negligible, the system aberration of the interferometer is not canceled because of the flipping of the wave front. Therefore in a single-pass configuration it is important to match the intensity to eliminate multiple reflections and to subtract the odd aberration from the resultant OPD mathematically. Besides, one should always align the reference surface to obtain a symmetric main interferogram.

In a double-pass configuration half of the reference surface is blocked. The test beam is reflected by the corner cube twice and by the reference surface once. The intensities of both the reference and the test beams match, and hence multiple-beam interference does not occur and an attenuator is not necessary. Because of the double reflection, the sensitivity of the double-pass configuration is twice that of the single-pass one. To ensure that the system aberration of the interferometer is canceled in a double-pass configuration, the corner cube should be placed as close to the reference surface as possible. Otherwise the wave front might change too much because of a long propagation. Therefore it is more accurate to test a corner cube or a right-angle prism in a double-pass configuration than in a single-pass configuration. It can be shown that all the derivations are correct for both the four-frame algorithm and the five-frame algorithm.[2,9] It can also be shown that for the double-pass configuration all the dihedral-angle equations[10,11] derived in a single-pass configuration are correct.

References and Notes

1. J. H. Bruning, J. E. Gallagher, D. P. Rosenfeld, A. D. White, D. J. Brangaccio, and D. R. Herriott, "Digital wavefront measuring interferometer for testing optical surfaces and lenses," Appl. Opt. **13,** 2693–2703 (1974).
2. J. Schwider, R. Burow, K.-E. Elssner, J. Grzanna, R. Spolaczyk, and K. Merkel, "Digital wave-front measuring interferometry: some systematic error sources," Appl. Opt. **22,** 3421–3432 (1983).
3. P. Hariharan, "Digital phase-stepping interferometry: effects of multiply reflected beams," Appl. Opt. **26,** 2506–2507 (1987).
4. C. Ai and J. C. Wyant, "Effect of spurious reflection on phase shift interferometry," Appl. Opt. **27,** 3039–3045 (1988).
5. G. Bonsch and H. Bohme, "Phase-determination of Fizeau interferences by phase-shifting interferometry," Optik **82,** 161–164 (1989).
6. R. A. Nicolaus, "Evaluation of Fizeau interferences by phase-shifting interferometry," Optik **87,** 23–26 (1991).
7. J. C. Wyant, "Use of an ac heterodyne lateral shear interferometry with real-time wavefront correction systems," Appl. Opt. **14,** 2622–2626 (1975).
8. In the right-hand side the main interference pattern has a many tilt fringes because of the term D; i.e., the phase of D term varies over the pupil. On the other hand, the phase of term F is equal to a constant over the pupil. Therefore the phase error approximately equals $\pm\sin^{-1}(F/D)$. For $R_1 = 4\%$ and $R_2 = 50\%$, phase error is $\pm 0.08\lambda$.
9. P. Hariharan, "Digital phase-stepping interferometry: a simple error-compensating phase calculation algorithm," Appl. Opt. **26,** 2504–2506 (1987).
10. D. A. Thomas and J. C. Wyant, "Determination of the dihedral angle errors of a corner cube from its Twyman–Green interferogram," J. Opt. Soc. Am. **67,** 467–472 (1977).
11. C. Ai and K. L. Smith, "Accurate measurement of the dihedral angle of a corner cube," Appl. Opt. **31,** 519–527 (1992).